Chemical Science

RSC Publishing

EDGE ARTICLE

View Article Online
View Journal | View Issue

Cite this: *Chem. Sci.*, 2013, **4**, 819

Concertedness in proton-coupled electron transfer cleavages of carbon–metal bonds illustrated by the reduction of an alkyl cobalt porphyrin†

Cyrille Costentin,* Guillaume Passard, Marc Robert and Jean-Michel Savéant*

Received 19th October 2012
Accepted 25th November 2012

DOI: 10.1039/c2sc21788k

www.rsc.org/chemicalscience

The cleavage of metal–oxygen or metal–carbon bonds is an essential step in the activation by transition metal complex catalysis of small molecules involved in the resolution of modern energy challenges. Deciphering the role of proton transfer as promoter of such reactions is an essential piece of knowledge in this connection, notably in establishing the degree of concertedness between the three associated events; electron transfer, proton transfer and bond breaking. The reductive cleavage of the cobalt–carbon bond of a tetraphenylporphyrin, reminiscent of vitamin B_{12} derivatives, is taken as an example. A systematic cyclic voltammetric analysis of the catalytic currents resulting from the reduction of the cobalt(II) porphyrin upon addition of an alkyl halide and an acid shows that, among all possible mechanisms, proton transfer and bond breaking are concerted but are not concerted with electron transfer.

Published on 28 November 2012 on http://pubs.rsc.org | doi:10.1039/C2SC21788K
Downloaded by SCD Université Paris 7 on 07 January 2013

Proton-coupled electron transfers (PCET) are the object of current active theoretical and experimental attention in view of their implication in a huge number of natural and synthetic processes.[1–5] Concerning the latter, particular interest is presently devoted to the electrochemistry of small molecules such as H_2, O_2, H_2O, and CO_2 in an effort to address contemporary energy challenges. In most cases activation of the electrochemistry of these small molecules requires catalysis, usually by means of high or low oxidation degrees of transition metal complexes. In these processes, proton transfer is not merely coupled with electron transfer but it is coupled with electron transfer and the breaking of a bond linking heavy atoms. In these catalytic processes, the coupling of PCET with bond breaking may then be of two kinds. It may concern the bond to be broken in the substrate like the O–O bond of dioxygen or one carbon–oxygen bond in CO_2, as it is also in the case with the direct electrochemical PCET–bond breaking reaction. It may also involve the bond that is transitorily established between the metal of the catalyst and a heavy atom, such as O or C, in the substrate.[6] So far, precise analyses of the mechanism and kinetics of a PCET–coupled bond breaking reaction have concerned a single instance, namely the direct electrochemical reduction of the O–O bond of an organic peroxide.[7] It was shown that, in this case, proton transfer, electron transfer and heavy-atom bond breaking are all concerted. On this occasion a kinetic model for this type of reaction was developed, which combines the model of concerted electron transfer–heavy-atom bond breaking reaction with the model of concerted PCET reactions (*i.e.* CPET reactions). As an example of a proton-promoted dissociative electron transfer of a heteroatom–metal bond in the framework of a catalyzed electrochemical reaction, we have selected the catalysis of the electrochemical reduction of an alkyl halide, chloroacetonitrile, by an electrogenerated cobalt(I) tetraphenylporphyrin, $Co^{I}TPP$ (Chart 1). As shown in Fig. 1, $Co^{II}TPP$ gives rise to a reversible cyclic voltammetric wave (upper Fig. 1) representing the reductive generation of the corresponding $Co^{I}TPP$ complex, which is stable in the time framework of slow scan cyclic voltammetry. The corresponding standard potential is $E^0_{Co^{II}/Co^{I}} = -0.785$ V *vs.* SCE. From the peak current, the diffusion coefficient may be estimated as $D_{TPPCo} = 4 \times 10^{-6}$ cm^2 s^{-1}.

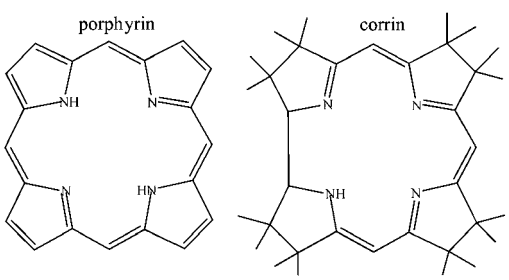

Chart 1

Univ Paris Diderot, Sorbonne Paris Cité, Laboratoire d'Electrochimie Moléculaire, Unité Mixte de Recherche Université - CNRS No 7591, Bâtiment Lavoisier, 15 rue Jean de Baïf, 75205 Paris Cedex 13, France

† Electronic supplementary information (ESI) available: Experimental details. Analysis of the all-concerted mechanism. See DOI: 10.1039/c2sc21788k

Published on 28 November 2012 on http://pubs.rsc.org | doi:10.1039/C2SC21788K
Downloaded by SCD Université Paris 7 on 07 January 2013

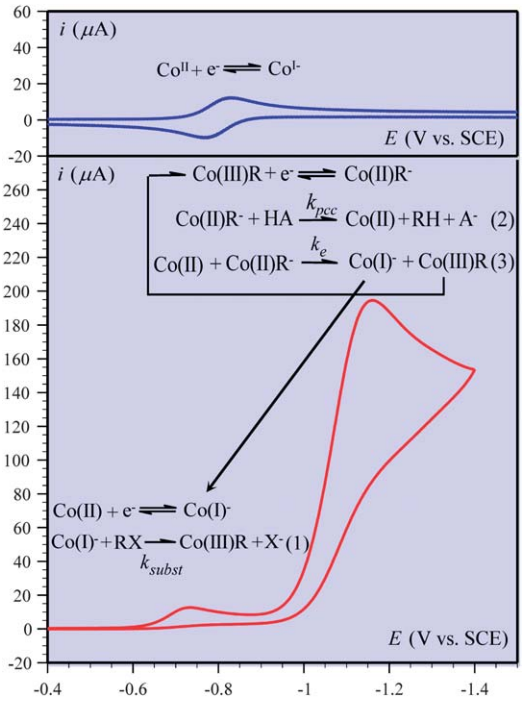

Fig. 1 Cyclic voltammetry of $Co^{II}TPP$ (1 mM) in DMF + 0.1 M *n*-NBu_4ClO_4 in the absence (upper diagram) and presence (lower diagram) of 50 mM $ClCH_2CN$ and 10 mM PhOH. Scan rate: 0.1 V s^{-1}. R = CH_2CN, X = Cl.

Upon addition of chloroacetonitrile and an acid, here phenol (lower Fig. 1), this wave becomes irreversible and a second wave appears at a more negative potential. The latter wave is much higher than the first, suggesting the occurrence of the catalytic sequence shown in Fig. 1.

The first step of the catalytic process is the alkylation of the $Co^{I}TPP$ produced by the electrochemical reduction of the starting $Co^{II}TPP$ yielding the $TPPCo^{III}R$ (R = CH_2CN) complex.[8] This reaction can also be observed at the level of the first wave, which is rendered irreversible according to an "EC" reaction scheme, where the "C" reaction is the Co^{I} alkylation reaction. Addition of increasing amounts of $ClCH_2CN$ results in an increasingly positive shift of the peak potential, E_p (Fig. 2a) as expected for an EC mechanism (Fig. 2a) from which the rate constant, k_{subst}, may be derived (Fig. 2b) according to:[9]

$$E_p = E^0_{Co^{II}/Co^{I}} - 0.78\frac{RT}{F} + \frac{RT\ln(10)}{2F}\log\left(\frac{RTk_{subst}[RX]}{Fv}\right) \quad (1)$$

(v is the scan rate). The slope, 27 mV per log unit, matches the occurrence of a pseudo-first order reaction following a fast electron transfer step. From the intercept and the value of the Co^{II}/Co^{I} standard potential one obtains, $k_{subst} = 1.9 \times 10^4$ M^{-1} s^{-1}.

With these parameters in hand, the catalytic process taking place at the second wave may now be analyzed. We first note that this reaction sequence involves the reductive cleavage of a $TPPCo^{III}R$ complex, which is reminiscent of the same reaction in Vitamin B_{12} derivatives[10–16] even though the corrin ring in B_{12} is somewhat different from the porphyrin ring considered here (Chart 1).

The results of a systematic investigation of the catalytic wave as a function of addition of an acid, phenol or acetic acid, are displayed in Fig. 3. In both cases, the catalytic current increases

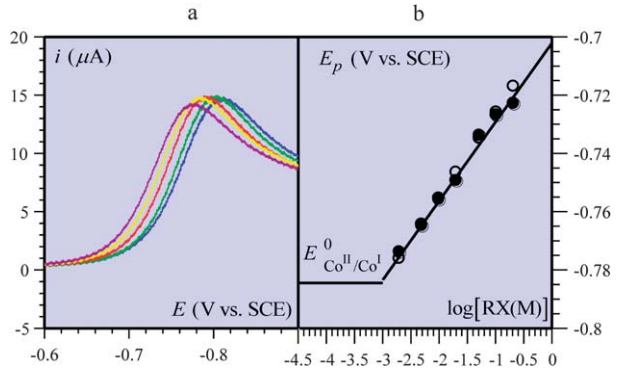

Fig. 2 Variation of the first wave with the concentration of $ClCH_2CN$. (a) Current–potential curves, from right to left: 1, 2, 5, 10, 20 mM. [$Co^{II}TPP$] = 1 mM in DMF + 0.1 M *n*-NBu_4ClO_4. Scan rate: 0.1 V s^{-1}. Temperature: 22 °C. (b) Full dots: experiments; open dots: value according to eqn (1).

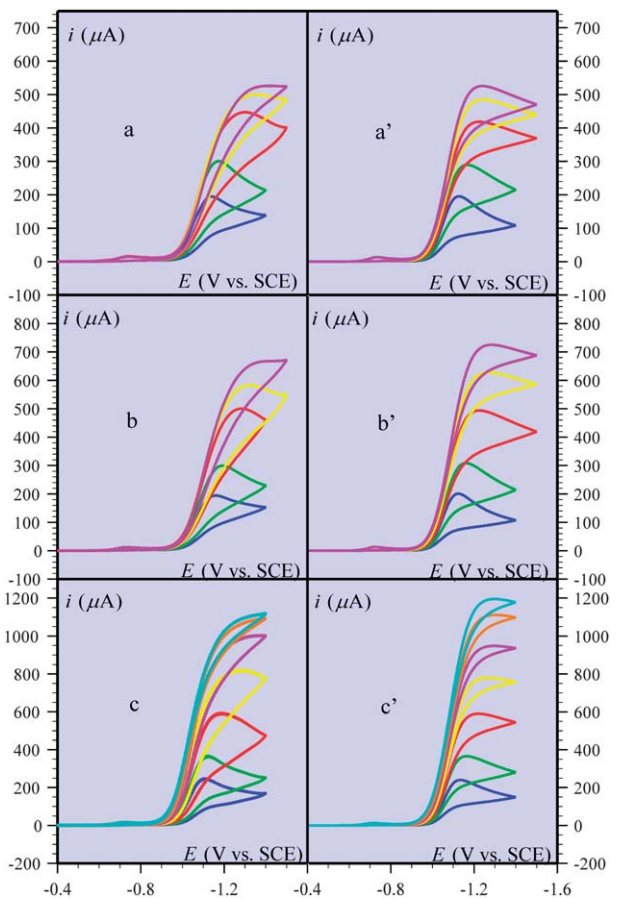

Fig. 3 Cyclic voltammetry of $Co^{II}TPP$ (1 mM) in DMF + 0.1 M *n*-NBu_4ClO_4 in the presence of: (a and a′) 50 mM $ClCH_2CN$ and increasing amount of phenol; (b and b′) 100 mM $ClCH_2CN$ and increasing amount of phenol; (c and c′) 200 mM $ClCH_2CN$ and increasing amount of acetic acid. Acid concentration (mM) 10 (blue), 20 (green), 50 (red), 100 (yellow), 200 (magenta), 500 (orange), 1000 (cyan). (a–c) Experimental. (a′–c′) Simulation (see text). Scan rate: 0.1 V s^{-1}.

This journal is © The Royal Society of Chemistry 2013

Published on 28 November 2012 on http://pubs.rsc.org | doi:10.1039/C2SC21788K
Downloaded by SCD Université Paris 7 on 07 January 2013

considerably upon acid addition as expected from the reaction sequence sketched in Fig. 1. The kinetics of the catalytic process is governed jointly by reactions (1) and (2), reaction (3) (see Fig. 1) being fast enough (close to the diffusion limit) to ensure that the steady state approximation applies to the $Co^{II}R^{-}$ intermediate.[17] If $ClCH_2CN$ and the acid were in sufficiently large concentrations for not being significantly consumed within the reaction-diffusion layer, one would expect the wave to be plateau-shaped.[18] This is indeed what tends to be observed for large $ClCH_2CN$ concentrations upon increasing the acid concentration (highest curves in Fig. 3). For lower acid concentrations, the wave is peak-shaped as expected for a non-negligible consumption of the acid. Relatively large concentrations of $ClCH_2CN$ were selected to examine the effect of acid addition in the largest possible concentration range. Upon raising the acid concentration, the increase of the catalytic wave levels off at a value that is dictated by the concentration of $ClCH_2CN$ as can be seen by comparing Fig. 3a–c. This observation falls in line with the fact that upon accelerating reaction (2) through acid addition, reaction (1) becomes the rate-determining step of the catalytic process. The maximal value of the quasi-plateau current thus obtained is proportional to $\sqrt{k_{pcc}[ClCH_2CN]}$ as expected when reaction (1) is rate-determining and the consumption of $ClCH_2CN$ is negligible, *i.e.* when:[18]

$$i_{plateau} = FS[Co^{II}TPP]\sqrt{D_{Co^{II}TPP}}\sqrt{k_{pcc}[ClCH_2CN]}$$

We may therefore simulate the experimental current–potential curves in Fig. 3 with the reaction sequence of Fig. 1.[19] Taking for the diffusion coefficients, $D_{TPPCoCH_2CN} \approx D_{Co^{II}TPP} = 4 \times 10^{-6}$, $D_{ClCH_2CN} = 10^{-5}$,[20] $D_{PhOH} \approx D_{PhO-} \approx D_{AcOH} \approx D_{AcO-} = 5 \times 10^{-6}$ cm^2 s^{-1},[21] adjustment of the various parameters led to the following values: $E^0_{Co^{III}R/Co^{II}R^-} = -1.05$ V *vs.* SCE, $k_S = 0.05$ cm s^{-1} (k_S is the standard rate constant for the $Co^{III}R/Co^{II}R^-$ couple, assuming a Butler–Volmer rate law with a 0.5 transfer coefficient[22]) and $k_{pcc}^{PhOH} \approx k_{pcc}^{AcOH} = 5 \times 10^4$ M^{-1} s^{-1}. Repeating the same experiments with deuterated phenol and acetic acid led to practically the same values of k_{pcc}. In the proton-coupled cleavage of the $Co^{II}R^-$ complex (reaction (2) in Fig. 1) the initial state is better viewed as an anion radical of the Co(II) porphyrin with the R moiety being present as the radical $R^\bullet$ by analogy with methyl cobinamide,[13a] as represented in Fig. 4. In the final state, the electron has been ultimately transferred onto $R^\bullet$ as the Co–C bond is broken. The reaction may thus be regarded as a proton-coupled electron transfer from the porphyrin π^* orbital to the σ^* Co–C orbital in which proton transfer and Co–C bond cleavage are concerted. The driving force of the reaction is quite large, 0.65 and 0.98 eV for PhOH and AcOH respectively,[23] leading to the representation of the potential energy profiles sketched in Fig. 4. Because of this large driving force, the transition state resembles the initial state, implying that the symmetry factor is very small. For the same reason proton tunneling in the transition state is quite easy, meaning that the reaction is adiabatic toward proton transfer. It follows that the magnitude of the reaction rate is

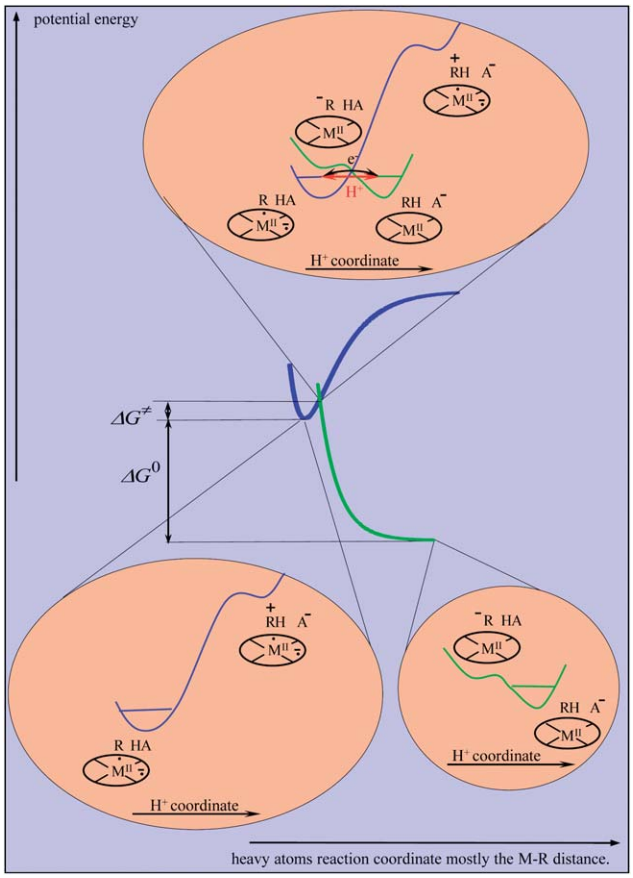

Fig. 4 Potential energy profiles for metal–carbon bond cleavage concerted with proton transfer. M is a metal center.

dictated by the non-adiabaticity of electron transfer. These considerations also explain why the rate constant is practically the same with PhOH and AcOH in spite of the difference in driving forces as well as the absence of a significant H/D kinetic isotope effect.

The mechanism in which electrode electron transfer is followed by a proton transfer concerted with Co–C bond cleavage thus matches the experimental facts. It is however necessary to examine the other mechanistic possibilities that are summarized in Scheme 1.

In all cases, the formation of Co^{II} is followed by a reaction that closes the catalytic loop (3) and by a reaction that regenerates the starting molecule by means of Co^{I} alkylation (1) as recalled in Scheme 1.

In the completely stepwise mechanism (blue pathway in Scheme 1), reaction (3) is so fast (at or close to the diffusion limit as already discussed) that it outruns the backward cleavage reaction. The cleavage reaction is thus the rate-determining step, which renders the overall kinetics insensitive to the next protonation step. The overall rate constant should therefore be insensitive to the acid concentration, contrary to experimental facts, and thus ruling out the possible occurrence of this pathway.

If the mechanism consisted of a concerted reductive cleavage followed by a protonation step (magenta pathway in Scheme 1),

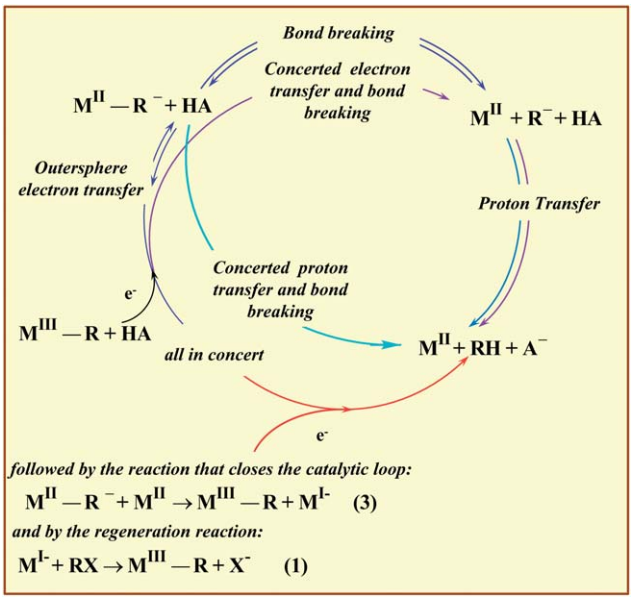

Scheme 1

the protonation step, following an irreversible step, would have no influence on the overall kinetics. The observed strong variation of the catalytic current with the addition of acid thus rules out this mechanism.

We examine finally the possible occurrence of a mechanism in which electron transfer, Co–C bond breaking and proton transfer would be concerted (red pathway in Scheme 1). When, at large $ClCH_2CN$ concentration, a plateau-shape is reached upon increasing acid concentration, the wave should shift toward positive potentials because the acid is then a reactant in the single-step termolecular reaction that involves, besides itself, the electrode and $ClCH_2CN$.[24] This is not observed experimentally (Fig. 3), ruling out this last mechanistic possibility.

We may thus conclude that in this proton-assisted reductive cleavage of the cobalt–carbon bond, bond breaking and proton transfer are concerted but that electron transfer is not concerted with these two events. This is not actually very surprising since the all-concerted pathway, being a termolecular reaction, would require a very large concentration of acid to compete. It is worth recalling in this connection that the only example recognized today of an all concerted electron–proton transfer bond cleavage involves the presence of an acid attached to the molecule being cleaved, equivalent to a very large local concentration.[7]

The above described reaction and the analysis of its mechanism is an illustrative example of a general problem, namely the detection and mechanism characterization of proton-coupled electron transfers as crucial steps of important catalytic processes involving coordination complexes. The present study has established a method to recognize the place of the proton-coupled electron transfer reaction within the catalytic process and to delineate its mechanism in the framework of the general reaction scheme shown in Scheme 1. The competition between the various pathways depends on a number of molecular and environmental parameters. It is too early to start establishing a general theory of such processes. It should indeed be borne in mind that the present system is merely the second in which the coupling between electron transfer, proton transfer and bond breaking has been analyzed. Although not our main goal, we also hope that the present findings will help future investigations of the reactivity and mechanisms in the reactions of methylcobalamin and coenzyme B_{12}.

Acknowledgements

Partial financial support from the Agence Nationale de la Recherche (ANR 2010 BLAN 0808) is gratefully acknowledged.

References and notes

1 (*a*) J. Stubbe, D. G. Nocera, C. S. Yee and M. C. Y. Chang, *Chem. Rev.*, 2003, **103**, 2167–2202; (*b*) S. Y. Reece, J. M. Hodgkiss, J. Stubbe and D. G. Nocera, *Philos. Trans. R. Soc. London, Ser. B*, 2006, **361**, 1351–1364.
2 J. L. Dempsey, J. R. Winkler and H. B. Gray, *Chem. Rev.*, 2010, **110**, 7024–7039.
3 S. Hammes-Schiffer and A. A. Stuchebrukhov, *Chem. Rev.*, 2010, **110**, 6939–6960.
4 J. J. Warren, T. A. Tronic and J. M. Mayer, *Chem. Rev.*, 2010, **110**, 6961–7001.
5 C. Costentin, M. Robert and J.-M. Saveant, *Chem. Rev.*, 2010, **110**, PR1–PR40.
6 (*a*) The two pathways may be competing as in the catalysis of dioxygen reduction leading to water and hydrogen peroxide respectively[6b]; (*b*) J. Rosenthal and D. G. Nocera, *Acc. Chem. Res.*, 2007, **40**, 543–553
7 C. Costentin, V. Hajj, M. Robert, J.-M. Saveant and C. Tard, *Proc. Natl. Acad. Sci. U. S. A.*, 2011, **108**, 8559–8564.
8 (*a*) By reference to the observations made with cobalt(I) porphyrins and cobalamins with several alkylating agents[8b–g]; (*b*) L. Smith, L. Mervyn, P. W. Muggleton, A. W. Johnson and N. Shaw, *Ann. N.Y. Acad. Sci.*, 1964, **112**, 564–574; (*c*) G. N. Schrauzer, E. Deutsch and R. L. Windgassen, *J. Am. Chem. Soc.*, 1968, **90**, 2441–2442; (*d*) M. Momenteau, M. Fournier and M. Rougée, *J. Chim. Phys.*, 1970, **67**, 926–931; (*e*) M. Momenteau and D. Lexa, *Biochem. Biophys. Res. Commun.*, 1974, **58**, 940–944; (*f*) M. Perrée-Fauvet, A. Gaudemer, P. Boucly and J. Devinck, *J. Organomet. Chem.*, 1976, **120**, 439–451; (*g*) D. Lexa, J.-M. Savéant and J. P. Soufflet, *J. Electroanal. Chem.*, 1979, **100**, 159–172
9 (*a*) L. Nadjo and J.-M. Savéant, *J. Electroanal. Chem.*, 1973, **48**, 113–145; (*b*) J.-M. Savéant, *Elements of molecular and biomolecular electrochemistry: an electrochemical approach to electron transfer chemistry*, John Wiley & Sons, Hoboken, NJ, 2006, Ch. 2, pp. 80–84.
10 (*a*) J. M. Pratt, *Inorganic Chemistry of Vitamin B_{12}*, Academic Press, New York, 1972; (*b*) ed. D. Dolphin, *B12*, John Wiley, New York, 1982, vol. I and II.

Published on 28 November 2012 on http://pubs.rsc.org | doi:10.1039/C2SC21788K
Downloaded by SCD Université Paris 7 on 07 January 2013

This journal is © The Royal Society of Chemistry 2013

Published on 28 November 2012 on http://pubs.rsc.org | doi:10.1039/C2SC21788K
Downloaded by SCD Université Paris 7 on 07 January 2013

11 (*a*) D. Lexa and J.-M. Savéant, *J. Am. Chem. Soc.*, 1978, **100**, 3220–3222; (*b*) D. Lexa and J.-M. Savéant, *Acc. Chem. Res.*, 1983, **16**, 235–243.
12 J. M. Pratt, in *Chemistry and Biochemistry of B12*, ed. R. Banerjee, John Wiley & Sons, New York, 1999.
13 (*a*) R. L. Birke, Q. Huang, T. Spataru and D. K. Gosser, *J. Am. Chem. Soc.*, 2006, **128**, 1922–1936; (*b*) T. Spataru and R. L. Birke, *J. Phys. Chem. A*, 2006, **110**, 8599–8604; (*c*) T. Spataru and R. L. Birke, *J. Electroanal. Chem.*, 2006, **593**, 74–86.
14 (*a*) O. Tinembart, L. Walder and R. Scheffold, *Ber. Bunsen-Ges.*, 1988, **92**, 1225–1231; (*b*) D. L. Zhou, O. Tinembart, R. Scheffold and L. Walder, *Helv. Chim. Acta*, 1990, **73**, 2225–2241; (*c*) D. L. Zhou, P. Walder, R. Scheffold and L. Walder, *Helv. Chim. Acta*, 1992, **75**, 995–1011.
18 (*a*) J.-M. Savéant and E. Vianello, in *Advances in Polarography*, ed. I. S. Longmuir, Pergamon Press, Cambridge, UK, 1st edn, 1959, vol. 1, p 367; (*b*) ref. 9b, pp. 106–119.
19 (*a*) Ref. 8b, pp. 121–125; (*b*) M. Rudolph, *J. Electroanal. Chem.*, 2003, **543**, 23–39.
20 A. Cardinale, A. A. Isse, A. Gennaro, M. Robert and J.-M. Savéant, *J. Am. Chem. Soc.*, 2002, **124**, 13533–13539.
21 C. Costentin, C. Louault, M. Robert and J.-M. Savéant, *Proc. Natl. Acad. Sci. U. S. A.*, 2009, **106**, 18143–18148.
22 Ref. 9b, ch. 1, pp. 30–32.
23 (*a*) The driving force of the reaction may be estimated as follows:

$$\Delta G^0_{Co^{II}R^- + AH \rightarrow Co^{II} + RH + A^-} = \left[FE^0_{Co^{II/I}} + \frac{RT\ln 10}{F}pK_{AH}\right] - \left[FE^0_{R^{\bullet/-}} + \frac{RT\ln 10}{F}pK_{RH}\right] + \Delta G^0_{Co^{II}R^- \rightarrow Co^{II} + R^{\bullet}}$$

$$\left[FE^0_{Co^{II/I}} + \frac{RT\ln 10}{F}pK_{AH}\right]_{DMF} = -0.785 + 0.0591 \times \left\{\begin{matrix}18.8\ (PhOH)\\ 13.3\ (AcOH)\end{matrix}\right\}^{23b} = \left\{\begin{matrix}0.326\ (PhOH)\\ 0.001(AcOH)\end{matrix}\right\}(eV)$$

$$\left[FE^0_{R^{\bullet/-}} + (RT\ln 10/F)pK_{RH}\right]_{DMF} \approx \left[FE^0_{R^{\bullet/-}} + (RT\ln 10/F)pK_{RH}\right]_{CH_3CN} = -0.72\ ^{23c} + 0.0591 \times 33.3\ ^{23d} = 1.249\ eV$$

$$\Delta G^0_{Co^{II}R^- \rightarrow Co^{II} + R^{\bullet}} = \Delta H^0_{Co^{II}R^- \rightarrow Co^{II} + R^{\bullet}} - T\Delta S^0_{Co^{II}R^- \rightarrow Co^{II} + R^{\bullet}} = 0.57^{23e} - 0.3 = 0.27\ eV$$

$$\Delta G^0_{Co^{II}R^- + AH \rightarrow Co^{II} + RH + A^-} = \left\{\begin{matrix}-0.652\ (PhOH)\\ -0.978(AcOH)\end{matrix}\right\}(eV);$$

15 (*a*) Particularly interesting in this connection is the finding that a nearby tyrosine accelerates Co–carbon bond homolysis in methylmalonyl-CoA mutase,[15b] suggesting coupling with proton transfer; (*b*) M. D. Vlasie and R. Banerjee, *J. Am. Chem. Soc.*, 2003, **125**, 5431–5435.
16 J. E. Arguello, C. Costentin, S. Griveau and J.-M. Savéant, *J. Am. Chem. Soc.*, 2005, **127**, 5049–5055.
17 The driving force of reaction (3) is: $E^0_{Co^{II}/Co^{I}} - E^0_{Co^{III}R/Co^{II}R^-} = 0.365$ V (see main text for the determination of $E^0_{Co^{III}R/Co^{II}R^-}$).
(*b*) C. P. Andrieux, J. Gamby, P. Hapiot and J.-M. Savéant, *J. Am. Chem. Soc.*, 2003, **125**, 10119–10124; J. Gamby, Thèse Université Paris-Diderot - Paris VII, 2003; (*c*) N. Bortolamei, A. A. Isse and A. Gennaro, *Electrochim. Acta*, 2010, **55**, 8312–8318; (*d*) K. Izutsu, *Acid–Base Dissociation Constants in Dipolar Aprotic Solvents*, Blackwell, 1990, pp. 17–35; (*e*) assuming that it is approximately the same as in methylcobalamin[13a]
24 A more rigorous demonstration is given in the ESI†.